

Table III. Comparison of Rate Constants for Substitution at In^{3+} (k_1) and at InOH^{2+} (k_2)

ligand	I, M	$k_1, M^{-1} s^{-1}$	$k_2, M^{-1} s^{-1}$
PAN ⁰	0.2	$\leq \sim 55^a$	$8 \times 10^4^a$
Hferron ^{+b}	0.2	1.1×10^3	
Ferron ^{0b}		9.7×10^4	1.2×10^7
murexide(1-) ^c	0.1	6.0×10^5	
SOX ^{-d}	0.1	2.8×10^5	
SO ₄ ^{2-e}	0	2.6×10^5	2.5×10^7
InOH ^{2+f}	0.5		4.1×10^5
H ₂ O ^g		2×10^4	

^aThis work, extrapolated. ^bReference 5. ^cKaway, Y.; Imamura, T.; Fujimoto, M. *Bull. Chem. Soc. Jpn.* **1975**, *48*, 3142-3145. Ohtani, Y.; Yagihashi, S. *Fujimoto, M. Ibid.* **1977**, *50*, 1345-1346. ^dSemixylenol orange: Kaway, Y.; Takahashi, T.; Hayashi, K.; Imamura, T.; Nakayama, H.; Fujimoto, M. *Bull. Chem. Soc. Jpn.* **1972**, *45*, 1417-1423. ^eMiceli, J.; Stuehr, J. *J. Am. Chem. Soc.* **1968**, *90*, 6967-6972. ^fReference 7. ^g k_1 in s^{-1} : Glass, G. E.; Schwabacher, W. B.; Tobias, R. S. *Inorg. Chem.* **1968**, *7*, 2471-2478.

Ti(III)¹⁴ and is usually ascribed to the labilization of the water molecules in the inner coordination sphere as a result of the hydrolysis. As has already been pointed out,¹⁵ the enhanced reactivity of the hydrolyzed species cannot be adduced as a criterion for the mechanism by which the *aquo* ion reacts.

In Table III we have collected the known forward rate constants for complex formation by In^{3+} and InOH^{2+} . The data cover a fairly wide range, which points in the direction of an associative mechanism.⁵ Nevertheless, the difference between the present results and those pertaining to all other ligands is quite striking and must have a specific reason. We suggest that an internal hydrogen-bond mechanism¹⁶ should be operative in this system.

Proton transfer to OH^- and general bases from internally hydrogen-bonded acids is known to proceed as well below the

- (14) Burgess, J. "Metal Ions in Solution"; Ellis Horwood Limited: Chichester, England, 1978; p 349.
 (15) Perlmutter-Hayman, B.; Tapuhi, E. *J. Coord. Chem.* **1979**, *9*, 177-183.
 (16) Mentasti, E.; Secco, F.; Venturini, M. *Inorg. Chem.* **1980**, *19*, 3528-3535 and references therein quoted.

"normal", diffusion-controlled rate.^{13,17,18} This feature is paralleled by an unusually slow rate of complex formation by substitution-labile cations such as Ni^{2+} , Co^{2+} , and Mg^{2+} , though the accelerating effect is absent for the more substitution-inert cations such as Al^{3+} . Among the possible mechanisms by which the internal hydrogen bond might slow down an otherwise rapid reaction, we can rule out rate-determining bond opening because in that case the plot of $1/\tau$ vs. c_M would not be a straight line. There remains the possibility that the hydrogen bond should be broken in a concerted attack by the cation; alternatively, the hydrogen-bonded form might be completely inactive and the cation react only with the nonbonded form present in small concentrations. The former explanation has been brought forward for the reaction between Ni^{2+} and substituted (phenylazo)resorcinols. It is interesting that NiOH^+ (which, in general, does not react significantly more rapidly than Ni^{2+} itself) forms the complex with these substances at a rate that is normal for Ni^{2+} . It was suggested that in this case the NiOH^+ acts as a strong base. On the other hand, InOH^{2+} is much less basic and it is not surprising that its rate should be slowed down to the same extent as that of In^{3+} .

Acknowledgment. We are indebted to the Italian CNR and the Kultusministerium Niedersachsen, West Germany, for financial support and to Prof. H. J. G. Hayman for programming the computer.

Registry No. PAN, 85-85-8; In, 7440-74-6.

- (17) Eigen, M.; Kruse, W.; Maas, G.; De Maeyer, L. *Prog. React. Kinet.* **1964**, *2*, 286.
 (18) (a) Diebler, H.; Secco, F.; Venturini, M. *J. Phys. Chem.* **1984**, *88*, 4229-4232. (b) Diebler, H.; Secco, F.; Venturini, M., to be submitted for publication in *J. Phys. Chem.*
 (19) Perlmutter-Hayman, B.; Shinar, R. *Inorg. Chem.* **1977**, *16*, 385-388.
 (20) Perlmutter-Hayman, B.; Shinar, R. *Inorg. Chem.* **1976**, *15*, 2932-2934.
 (21) In this paper the periodic group notation is in accord with recent actions by IUPAC and ACS nomenclature committees. A and B notation is eliminated because of wide confusion. Groups IA and IIA become groups 1 and 2. The d-transition elements comprise groups 3 through 12, and the p-block elements comprise groups 13 through 18. (Note that the former Roman number designation is preserved in the last digit of the new numbering: e.g., III \rightarrow 3 and 13.)

Contribution from the Department of Chemistry, Faculty of Science, Tohoku University, Aoba, Aramaki, Sendai 980, Japan

Mechanism of Acid-Catalyzed Decomposition of the $(\Delta\Delta, \Lambda\Lambda)$ - $(\mu\text{-Hydroxo})(\mu\text{-peroxo})\text{bis}[\text{bis}(\text{ethylenediamine})\text{cobalt(III)}]$ Ion

MASAHIRO EBHARA, YOICHI SASAKI, and KAZUO SAITO*¹

Received November 14, 1984

The change in the absorption spectrum accompanied by the decomposition of the title ion to cobalt(II) ions and dioxygen in perchloric acid solution, $[\text{H}^+] = 0.01\text{--}1.5 M$, takes place in two stages. The initial stage is completed within the stopped-flow mixing time (< 5 ms) and corresponds to protonation equilibrium (protonation constant $\sim 10 M^{-1}$, $M = \text{mol dm}^{-3}$, at $5\text{--}45^\circ\text{C}$ and $I = 1.0\text{--}3.0 M$). The protonated species exhibits an absorption maximum at ca. 520 nm. The second slow stage enables kinetic studies in $0.01\text{--}0.20 M$ HClO_4 to be made, the observed rate constants being $0.02\text{--}0.3 s^{-1}$ at 35°C and $I = 1.0 M$. The decomposition seems to proceed exclusively from the protonated species through the cleavage of the hydroxide bridge to give a singly bridged $\mu\text{-peroxo}$ binuclear cobalt(III) complex $[(\text{en})_2(\text{H}_2\text{O})\text{Co}^{\text{III}}(\mu\text{-O}_2^{2-})\text{Co}^{\text{III}}(\text{H}_2\text{O})(\text{en})_2]^{4+}$, which subsequently undergoes deoxygenation.

The $(\mu\text{-peroxo})(\mu\text{-hydroxo})\text{bis}[\text{bis}(\text{ethylenediamine})\text{cobalt(III)}]$ ion, $[(\text{en})_2\text{Co}^{\text{III}}(\mu\text{-OH})(\mu\text{-O}_2^{2-})\text{Co}^{\text{III}}(\text{en})_2]^{3+}$ (**1**), undergoes proton-assisted decomposition into dioxygen and cobalt(II) species in the pH region from 1 to 3.5.^{2,3} No $[\text{H}^+]$ dependence was

observed for the decomposition of the singly bridged $\mu\text{-peroxo}$ dicobalt(III) complexes such as $[(\text{en})_2\text{NH}_3\text{Co}^{\text{III}}(\mu\text{-O}_2^{2-})\text{Co}^{\text{III}}\text{NH}_3(\text{en})_2]^{4+}$ over a wide pH range from 1.1 to 10.⁴⁻⁸

- (1) Present address: Coordination Chemistry Laboratories, Institute for Molecular Science, Myodaiji, Okazaki 444, Japan.
 (2) Zehnder, M.; Macke, H.; Fallab, S. *Helv. Chim. Acta* **1975**, *58*, 2306-2312.
 (3) Al-Shatti, N.; Ferrer, M.; Sykes, A. G. *J. Chem. Soc., Dalton Trans.* **1980**, 2533-2535.
 (4) Simplicio, J.; Wilkins, R. G. *J. Am. Chem. Soc.* **1969**, *91*, 1325-1329.
 (5) Ferrer, M.; Hand, T. D.; Sykes, A. G. *J. Chem. Soc., Dalton Trans.* **1980**, 14-18.
 (6) Sasaki, Y.; Suzuki, K. Z.; Matsumoto, A.; Saito, K. *Inorg. Chem.* **1982**, *21*, 1825-1828.
 (7) Kanesato, M.; Ebihara, M.; Sasaki, Y.; Saito, K. *J. Am. Chem. Soc.* **1983**, *105*, 5711-5713.

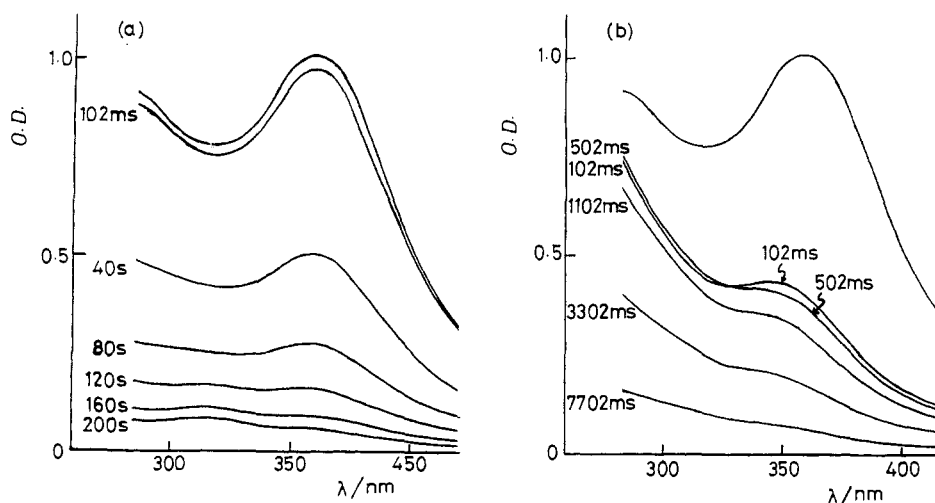


Figure 1. Change in absorption spectra on mixing aqueous solutions of $[(en)_2Co^{III}(\mu-OH)(\mu-O_2^{2-})Co^{III}(en)_2]^{3+}$ with perchloric acid: (a) $[H^+] = 0.01$ M; (b) $[H^+] = 1.5$ M. $[Co^{III}] = 2.00 \times 10^{-4}$ M, $I = 3.0$ M ($NaClO_4$), $25^\circ C$. Top lines are spectra in neutral solution.

Kinetic analysis^{2,3,9} of the deoxygenation of both meso and racemic isomers of **1** revealed rapid establishment of a protonation equilibrium (reported protonation constant of the meso isomer is $4.16 M^{-1}$ ($M = mol\ dm^{-3}$) at $20^\circ C$ and $I = 1.15$ M (KCl)² and is $15.6 M^{-1}$ at $25^\circ C$ and $I = 0.2$ M ($NaClO_4$)³ and succeeding decomposition of the protonated species. The decomposition was claimed to occur through hydroxide bridge cleavage.^{3,9,10}

There are two possible protonation sites, peroxide and hydroxide ions.^{3,9,10} Protonation at the peroxide bridge has been considered more plausible.^{3,10} Rapid protonation equilibria at the hydroxide bridge have been reported prior to the bridge cleavage of some dicobalt(III) complexes such as $[(NH_3)_3Co^{III}(\mu-OH)_3Co^{III}(\mu-OH)_3]^{3+}$ and $[(nta)Co^{III}(\mu-OH)_2Co^{III}(nta)]^{2-}$ ($nta =$ nitrilotriacetate). The protonation constants obtained from kinetic analysis are 1.51^{11} and $42.8 M^{-1}$,¹² respectively.

It has been pointed out that the spectral pattern of **1** is similar to that of $[(en)_2Co^{III}(\mu-NH_2)(\mu-O_2^{2-})Co^{III}(en)_2]^{3+}$ and is reckoned to be characteristic of doubly bridged structures.¹³ It is expected that the overall pattern of the absorption spectrum should remain unchanged if the protonation took place at the hydroxide bridge of **1**. However, the absorption spectrum of $[(en)_2Co^{III}(\mu-NH_2)(\mu-O_2^{2-})Co^{III}(en)_2]^{3+}$, which does not undergo decomposition, changes significantly on protonation. The spectrophotometrically obtained protonation constant is $6.8 M^{-1}$ at $25^\circ C$ and $I = 0.245$ M ($NaClO_4$).¹⁴ Since the μ -peroxide moiety is the unique protonation site, this observation must reflect the formation of a hydroperoxide bridge.

We have reinvestigated the decomposition of $[(en)_2Co^{III}(\mu-OH)(\mu-O_2^{2-})Co^{III}(en)_2]^{3+}$ (**1**) over an extended $[H^+]$ range, 0.01–1.5 M, by use of a pure racemic mixture. The nature of the protonated complex was clarified by rapid-scanning ultraviolet spectrophotometry, and the mechanism of decomposition was discussed on the basis of kinetic studies.

Experimental Section

(1) Materials. The racemic perchlorate of **1** was prepared by modifying the reported method.¹⁵ Oxygen was slowly introduced into ethanol

(1:1–1:2, v/v) solution of cobalt(II) perchlorate hexahydrate (0.2 M) and ethylenediamine (ca. 0.5 M) either at room temperature or at $0^\circ C$ for 30 min to 3 h, and a black crystalline precipitate was collected. The solid was a mixture of meso and racemic forms (vide infra). Pure racemate was obtained by keeping the filtrate of the first crop in a refrigerator for at least 10 h. The yield was low and not always reproducible. The racemate was reckoned to be pure whenever the first-order plot of its decomposition (at 356 nm) in acid solution into Co^{II} and O_2 was linear over 90% of the decomposition. The first-order rate constant was $8.8 \times 10^{-3} s^{-1}$ in 0.01 M HCl solution at $20^\circ C$ and $I = 0.15$ M (KCl), and is compared to the reported value $1.2 \times 10^{-2} s^{-1}$ under a similar condition.² Our value was reproducible among independently prepared samples.¹⁶ The racemate shows absorption peaks at 356 ($\epsilon = 5620 M^{-1} cm^{-1}$) and 276 nm (5130) in aqueous solution at $25^\circ C$, in reasonable agreement with the reported values.¹⁷

Special grade sodium perchlorate and perchloric acid (Kanto Chemicals) were used without further purification.

(2) Measurements. Ultraviolet and visible absorption spectra were recorded with a Hitachi 330 spectrophotometer. A Union Giken RA-401 stopped-flow spectrophotometer was used for rapid-scanning spectroscopy and kinetic studies at 35 – $50^\circ C$. A Hitachi 330 spectrophotometer and a Union Giken MX7 rapid-mixing apparatus were used for kinetic runs at $5^\circ C$.

Results

Our observation is summarized as follows. The reaction proceeds through two stages. The "rapid stage" completed within 5 ms and seems to correspond to the protonation. The following "slow stage" corresponds to the decomposition of the binuclear species. The rapid stage was studied by rapid-scanning spectroscopy at relatively high H^+ concentration (0.1–1.5 M) to obtain the protonation constant and the absorption spectrum of protonated species. The slow stage was studied kinetically at $[H^+] = 0.01$ – 0.2 M. Both studies were performed in perchlorate media.

(1) Overall Change in Absorption Spectrum during the Decomposition. Figure 1 shows the change in absorption spectra in the region from 270 to 450 nm on mixing a neutral aqueous solution of racemic **1** with perchloric acid. The spectra immediately after mixing at both $[H^+] = 0.01$ and 1.5 M are more or less different from that of **1** in neutral solution. The rapid stage should be completed within the dead time (30 ms) of the apparatus and even within 5 ms at $35^\circ C$, since it was not followed by the stopped-flow technique.

(8) Sasaki, Y.; Tachibana, M.; Saito, K. *Bull. Chem. Soc. Jpn.* **1982**, *55*, 3651–3652.

(9) Fallab, S.; Zehnder, M.; Thewalt, U. *Helv. Chim. Acta* **1980**, *63*, 1491–1498.

(10) Fallab, S.; Mitchell, P. R. *Adv. Inorg. Bioinorg. Mech.*, in press.

(11) Edwards, J. D.; Wieghardt, K.; Sykes, A. G. *J. Chem. Soc., Dalton Trans.* **1974**, 2198–2204.

(12) Melson, D. R.; Harris, G. M. *Inorg. Chem.* **1977**, *16*, 434–437.

(13) Sasaki, Y.; Fujita, J.; Saito, K. *Bull. Chem. Soc. Jpn.* **1971**, *44*, 3373–3378.

(14) Mori, M.; Weil, J. A. *J. Am. Chem. Soc.* **1967**, *89*, 3732–3744. Mori, M.; Weil, J. A.; Ishiguro, M. *Ibid.* **1968**, *90*, 615–621.

(15) Foong, S. W.; Miller, J. D.; Oliver, F. D. *J. Chem. Soc. A* **1969**, 2847–2850.

(16) The reported decomposition rate constant for the meso form is $5.8 \times 10^{-2} s^{-1}$,² which is larger by ca. 5 times than the reported value for the racemic form. Some of our samples gave curved first-order plots with faster initial decrease of absorbance than the that of pure racemate. The initial rapid decrease should correspond to the meso isomer.

(17) Cabani, S.; Ceccanti, N.; Conti, G. *J. Chem. Soc., Dalton Trans.* **1983**, 1247–1251.

Table II. Kinetic Data for the Proton-Assisted Deoxygenation of [(en)₂Co^{III}(μ-OH)(μ-O₂²⁻)Co^{III}(en)₂]³⁺ ^a

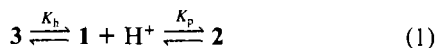
isomer	I/M	media	t/°C	B/M ⁻¹ ^b	A/s ⁻¹ ^c	ref
racemic	1.0	NaClO ₄	5.0	3.4 ± 0.2	0.079 ± 0.001	d
racemic	1.0	NaClO ₄	35.0	3.0 ± 0.2	2.35 ± 0.01	d
racemic	1.0	NaClO ₄	40.0	3.2 ± 0.2	3.86 ± 0.04	d
racemic	1.0	NaClO ₄	45.0	3.2 ± 0.2	6.58 ± 0.02	d
racemic	3.0	NaClO ₄	5.0	8 ± 1	0.151 ± 0.004	d
meso	0.2	NaClO ₄	25.0	15.6 ± 1.7	2.07 ± 0.012	e
meso	1.15	KCl	20	32	7.68 ± 0.01	f
meso	1.0	KCl	25	31.3	14.4	g
racemic	1.0	KCl	25	15.4	2.46	g

^ak_{obs} = A[H⁺]/(1 + B[H⁺]). ^bSee text. B = K_p + K_h. ^cSee text. A = k₃K_h. ^dThis study. ^eReference 3, data recalculated by the formulas given in footnotes b and c. ^fReference 2; data similarly recalculated. ^gData by Fallab et al. cited in ref 3 and recalculated similarly.

The rapid stage was followed by a monotonous decrease in absorbance at [H⁺] = 0.01 M, which was completed within 400 s. At [H⁺] = 1.5 M, the slow stage involves two steps; the absorbance between 280 and 340 nm first increased and then decreased monotonously within 20 s. Nevertheless the final spectra correspond to that of cobalt(II) ions over the whole pH range.

In hydrochloric acid (0.5–3.0 M) the overall pattern of change is similar to that in perchloric acid. The final spectra, however, indicate that the products contain some uninuclear cobalt(III) complex and some μ-superoxo binuclear cobalt(III) complex identified by a peak at ca. 700 nm¹⁸ as well as cobalt(II). The yield of uninuclear cobalt(III) species and μ-superoxo complex seems to increase with an increase in HCl concentration. The two-step change in the absorption spectra in the slow stage is more distinctive in HCl than in HClO₄. The first (increase in absorbance in the 285 nm-region) and the second step (decrease in the region) were completed within 10 and 400 s respectively in 1.5 M HCl solution at I = 3.0 M (LiCl). The increase in absorbance at ca. 700 nm is seen in the second step only.

(2) Rapid Protonation Equilibrium. The absorption spectrum immediately after mixing depends significantly on [H⁺]. The extent of deviation from the spectrum in neutral solution is larger at higher proton concentrations. The spectra at the end of rapid stage were analyzed in various H⁺ concentrations on the basis of eq 1. Since there are two sites where a proton can reside in the



initial complex **1**, the protonated species at the peroxide and the hydroxide moiety are designated by **2** and **3**, and their protonation constants by K_p and K_h. The concentrations of the total complex [c]_t of **1**, **2**, and **3** are related to the observed molar extinction coefficient ε_{app} by eq 2, where ε₁, ε₂, and ε₃ represent molar ex-

$$\epsilon_{app}[c]_t = \epsilon_1[c]_1 + \epsilon_2[c]_2 + \epsilon_3[c]_3 \quad (2)$$

tinction coefficients of **1**, **2**, and **3**, respectively. When the protonation constants for the formation of **2** and **3** are expressed by K_p and K_h, respectively, eq 2 is rewritten as eq 3. Since [c]_t =

$$\epsilon_{app}[c]_t = \epsilon_1[c]_1 + \epsilon_2[c]_1[H^+]K_p + \epsilon_3[c]_1[H^+]K_h \quad (3)$$

[c]₁ + K_p[c]₁[H⁺] + K_h[c]₁[H⁺], eq 3 is re-formed as eq 4 and 5. Taking reciprocals of both sides of eq 5, eq 6 is obtained. The

$$\epsilon_{app}[1 + (K_p + K_h)[H^+]] = \epsilon_1 + [[H^+](\epsilon_2K_p + \epsilon_3K_h)] \quad (4)$$

$$\epsilon_{app} - \epsilon_1 =$$

$$[(\epsilon_2 - \epsilon_1)K_p + (\epsilon_3 - \epsilon_1)K_h][H^+]/[1 + (K_p + K_h)[H^+]] \quad (5)$$

$$\frac{1}{\epsilon_1 - \epsilon_{app}} =$$

$$\frac{1}{(\epsilon_1 - \epsilon_2)K_p + (\epsilon_1 - \epsilon_3)K_h} \frac{1}{[H^+]} + \frac{K_p + K_h}{(\epsilon_1 - \epsilon_2)K_p + (\epsilon_1 - \epsilon_3)K_h} \quad (6)$$

plots 1/(ε₁ - ε_{app}) vs. 1/[H⁺] gave a straight line. From the ratio

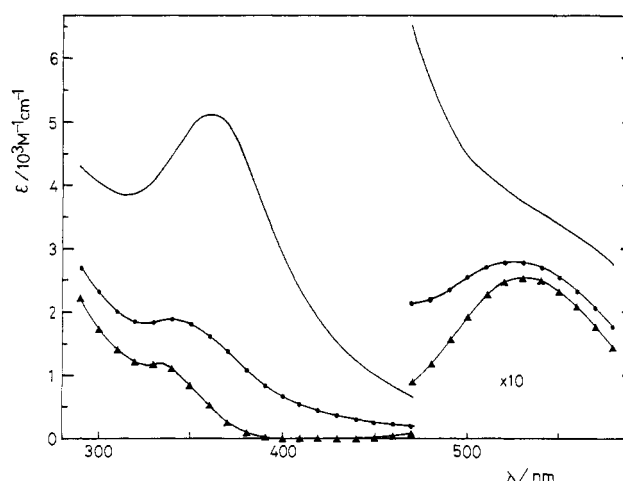


Figure 2. Absorption spectra of the protonated species of [(en)₂Co^{III}(μ-OH)(μ-O₂²⁻)Co^{III}(en)₂]³⁺ calculated from those in acid solutions on the basis of eq 3 (I = 3.0 M, 25 °C): (—) in neutral solution; (●) on the assumption ε₁ = ε₃ and K_h = 0; (▲) on the assumption ε₁ = ε₃ and ε₂ > 0.

of its intercept to the gradient the sum of K_p and K_h can be calculated. (ε₁ was obtained experimentally, vide supra.) Since the data do not give the contribution of the [H⁺]² term, simultaneous protonation on both the μ-hydroxo and μ-peroxo moieties was not taken into consideration. By use of ε₁ and ε_{app} values at 520, 440, 360, and 340 nm, the K_p + K_h values were obtained to be 7.7 ± 0.6, 7.7 ± 0.6, 8.1 ± 0.8, and 7.7 ± 0.6 M⁻¹, respectively, at 25 °C and I = 3.0 M (NaClO₄) (average 7.8 ± 0.7 M⁻¹).

When ε₃ is assumed not to be very different from ε₁, the gradient of eq 6 is expressed by 1/(ε₁ - ε₂)K_p. Since ε₂ > 0, K_p should be greater than the reciprocal of the product ε₁[gradient]. When the lowest limit value of K_p is estimated on the basis of observed spectral data, the value at 400–420 nm is the biggest and 6.0 < K_p < 7.8 M⁻¹. Figure 2 shows the absorption spectra obtained by plotting the ε₂ values at various wavelengths by use of the lower and upper limit of K_p values. They correspond to the absorption spectrum of the μ-O₂H form given under the estimated K_p values. They are similar to each other in pattern and indicate clearly that this form of the protonated complex has a maximum at ~520 nm.

(3) Kinetics for the Slow Stage. This stage was kinetically analyzed at [H⁺] = 0.01–0.20 M, I = 1.0 and 3.0 M, and 5.0–45.0 °C, where the reaction proceeds as a single step. The reaction was monitored at 356 nm, and the initial concentration of complex was 1.6 × 10⁻⁴ M. The first-order plot was linear up to 90% completion of the absorption change. All the k_{obsd} values are listed in Table I (supplementary material). The plot of k_{obsd}⁻¹ vs. [H⁺]⁻¹ gives a very good straight line in the given acid concentration range. The rate law (7) is in accord with the experimental results.

$$k_{obsd} = A[H^+]/(1 + B[H^+]) \quad (7)$$

Since the data do not give the contribution of the [H⁺]² term, simultaneous protonation on both the μ-hydroxo and μ-peroxo moiety was not taken into consideration. Table II gives the

observed *A* and *B* values. The apparent ΔH^\ddagger and ΔS^\ddagger values for *A* are $78.4 \pm 0.6 \text{ kJ mol}^{-1}$ and $16.3 \pm 1.9 \text{ J mol}^{-1} \text{ K}^{-1}$, respectively. The *B* value does not give appreciable temperature dependence.

Discussion

(1) The Rapid Stage. The change in absorption spectra in the rapid stage ($>10^3 \text{ s}^{-1}$) is too fast to be accounted for by a breaking or formation of a coordination bond on cobalt(III)¹⁹ and should correspond to simple protonation. The spectrum of **2** in the 300–600-nm region is similar to those of the μ -hydroperoxo complexes $[(\text{en})_2\text{Co}^{\text{III}}(\mu\text{-NH}_2)(\mu\text{-O}_2\text{H}^{(-)})\text{Co}^{\text{III}}(\text{en})_2]^{4+}$ with an absorption maximum at 488 nm ($\epsilon = 347 \text{ M}^{-1} \text{ cm}^{-1}$)¹⁴ and $[(\text{NH}_3)_5\text{Co}^{\text{III}}(\mu\text{-O}_2\text{H}^{(-)})\text{Co}^{\text{III}}(\text{NH}_3)_5]^{5+}$ with a peak at 492 nm ($\epsilon = 119 \text{ M}^{-1} \text{ cm}^{-1}$).⁵ Hence the absorption spectrum at the end of the first stage (lower lines in Figure 2) should represent that of **2**.

The sum of K_p and K_h was obtained as shown in the Results, but further discussion on individual K_p and K_h values is not made from the present experiment.

(2) The Slow Stage. Kinetics in the past have been based on the assumption that only one protonation site is available on the substrate complex. However, neither **2** nor **3** can be excluded from the discussion as shown in the Results. The following discussion takes all the species, **1**, **2**, and **3**, into consideration as precursors for the decomposition. k_{obsd} can be expressed by eq 8 where k_1 ,

$$k_{\text{obsd}} = \frac{k_1 + (k_2K_p + k_3K_h)[\text{H}^+]}{1 + (K_p + K_h)[\text{H}^+]} \quad (8)$$

k_2 , and k_3 represent the first-order decomposition rate constants of **1**, **2**, and **3**, respectively. Since the decomposition does not take place in neutral solutions, k_1 is reckoned to be zero, and this is supported by the experimental formula (7). The term *B* in eq 7 is expressed by $(K_p + K_h)$, and its value at $I = 3.0 \text{ M}$ is in good agreement with that obtained spectroscopically ($7.8 \pm 0.7 \text{ M}^{-1}$). This coincidence provides an evidence for the legitimacy of the treatment.

The protonated species **2** should not be the precursor for decomposition but provides a dead end, because it is known that the protonated form of the singly bridged complex $[(\text{NH}_3)_5\text{Co}^{\text{III}}(\mu\text{-O}_2^{(2-)})\text{Co}^{\text{III}}(\text{NH}_3)_5]^{4+}$ is not reactive⁵ and that the doubly bridged complex $[(\text{en})_2\text{Co}^{\text{III}}(\mu\text{-NH}_2)(\mu\text{-O}_2^{(2-)})\text{Co}^{\text{III}}(\text{en})_2]^{3+}$ fails to undergo deoxygenation both in the original and protonated forms.¹⁴ Hence we consider that k_2 is also reckoned to be zero. Since **3** is converted into a singly bridged μ -peroxo complex, it should be the unique precursor for decomposition.

Another interpretation may be encountered by considering that protonation of **1** takes place at the peroxide moiety to give **2** and the proton is transferred to the hydroxide bridge. This scheme does not seem convincing because studies with molecular models indicate that the proton on the peroxide may locate in a position remote from the hydroxide part of the bridge, and there seems to be difficulty in tossing the proton from O_2^{2-} to OH^- .

Equation 8 is reduced to eq 9. Since the upper limit of K_h is 1.8 M^{-1} , k_3 must be greater than 0.45 s^{-1} at 25°C and $I = 1.0 \text{ M}$.

$$k_{\text{obsd}} = \frac{k_3K_h[\text{H}^+]}{1 + (K_p + K_h)[\text{H}^+]} \quad (9)$$

The overall scheme may be written as shown in Figure 3. The aqua-bridged species **3** undergoes cleavage of Co–O bonds to give a singly bridged **4**, which further undergoes intramolecular electron transfer to give cobalt(II) and O_2 .

Further analysis of kinetic data to estimate individual values of k_a , k_b , and k_c cannot be realized. If k_c were rate determining, k_c should be greater than 0.45 s^{-1} . If k_a were rate determining, k_c should be greater. We have discussed that the rate of de-

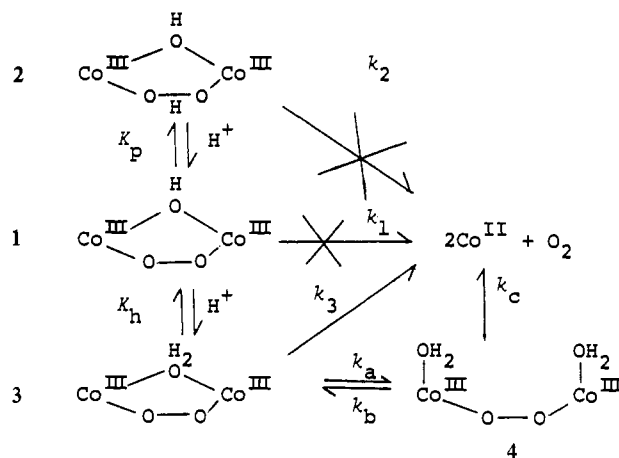


Figure 3. Proposed reaction scheme in the slow stage of spectral change on mixing **1** with acid. (The protonated precursor **3** undergoes deoxygenation in two steps.)

composition of binuclear cobalt(III) complexes singly bridged by peroxide is ruled by the ease with which the electron in the peroxide moiety is transferred to cobalt(III).⁷ The first-order rate constant for the decomposition of $[(\text{en})_2(\text{NH}_3)\text{Co}^{\text{III}}(\mu\text{-O}_2^{(2-)})\text{Co}^{\text{III}}(\text{NH}_3)(\text{en})_2]^{4+}$ and $[(\text{NH}_3)_5\text{Co}^{\text{III}}(\mu\text{-O}_2^{(2-)})\text{Co}^{\text{III}}(\text{NH}_3)_5]^{4+}$ are 4.8×10^{-3} and 84 s^{-1} at 25°C and $I = 0.1 \text{ M}$, respectively.^{5,6} The rate seems to be very sensitive to the ligand around cobalt(III).

If k_a were rate determining, $k_a = k_3$ and the value is unusually great for a substitution-inert cobalt(III) species. (If k_c were rate determining the k_a value would be greater.) Rapid anation on $[(\text{salen})(\text{H}_2\text{O})\text{Co}^{\text{III}}(\mu\text{-O}_2^{(2-)})\text{Co}^{\text{III}}(\text{H}_2\text{O})(\text{salen})]$ (*salen* = bivalent anion of bis(salicylaldehyde)ethylenediamine) was lately pointed out, but accounted for by the labilizing effect of *salen* rather than the bridging peroxide.²⁰ The present result seems to be the first example demonstrating labilization by bridging peroxide.

In 1.5 M HClO_4 , where the decrease in absorption intensity between 240 and 370 nm proceeds in two steps and fails to follow the first-order rate law, the kinetic analysis was made with difficulty. The complicated change in spectral pattern with time may be interpreted by considering another protonation on **4** to result in a dead end with respect to the decomposition to cobalt(II) and oxygen and/or the formation of other species than them. Such influence of protons was not apparent in $[\text{H}^+] < 0.2 \text{ M}$ but becomes appreciable with an increase in $[\text{H}^+]$ concentration.

(3) In Hydrochloric Acid Solution. The product is different from that in perchloric acid. The steps for the formation of **2** and **3** and the breaking of Co–O bond to give **4** can be common. The singly bridged product, however, may have a slightly different structure such as $[(\text{en})_2(\text{H}_2\text{O})\text{Co}^{\text{III}}(\mu\text{-O}_2^{(2-)})\text{Co}^{\text{III}}\text{Cl}(\text{en})_2]^{3+}$ (**5**).²¹ **5** or its protonated form may be less reactive to electron transfer from peroxide to cobalt(III) and may undergo cleavage of the Co^{III}–O bond in a different manner to give $[\text{Co}^{\text{III}}(\text{en})_2(\text{H}_2\text{O})_2]^{3+}$ and/or binuclear Co^{III} complexes bridged by superoxide. The formation mechanism of the latter is unknown, but a disproportionation pathway is suggested.¹⁰ This view is supported by the following observation. First, the yield of uninnuclear Co^{III} species and binuclear complex bridged by superoxide increases with an increase in acid concentration. Second, the singly bridged complex $[(\text{en})_2(\text{NH}_3)\text{Co}^{\text{III}}(\mu\text{-O}_2^{(2-)})\text{Co}^{\text{III}}(\text{NH}_3)(\text{en})_2]^{4+}$ gives uninnuclear and superoxo-bridged species rather than cobalt(II) and O_2 in both hydrochloric and perchloric acid solutions of $[\text{H}^+] > 1.0 \text{ M}$. The ease with which protonated **5** undergoes disproportionation or Co^{III}–O bond cleavage should depend on the ligands on cobalt(III).

Acknowledgment. This work was supported by a Grant-in-Aid for Special Project Research (No. 57102001) to K.S. from the

(19) The reported greatest value for the second-order rate constant with respect to the complex and proton for the cleavage of a hydroxo bridge between two Co^{III} ions is $1.01 \text{ M}^{-1} \text{ s}^{-1}$ for the ternary bridged complex $[(\text{NH}_3)_3\text{Co}^{\text{III}}(\mu\text{-NH}_2)(\mu\text{-OH})_2\text{Co}^{\text{III}}(\text{NH}_3)_3]^{3+}$.¹¹

(20) Au-Yeung, S. C. F.; Eaton, D. R. *Inorg. Chem.* **1984**, *23*, 1517–1520.

(21) The cleavage of the hydroxo bridge of $[(\text{NH}_3)_5\text{Co}^{\text{III}}(\mu\text{-NH}_2)(\mu\text{-OH})\text{Co}^{\text{III}}(\text{NH}_3)_4]^{4+}$ in diluted hydrochloric acid gives $[(\text{NH}_3)_4(\text{H}_2\text{O})\text{Co}^{\text{III}}(\mu\text{-NH}_2)\text{Co}^{\text{III}}\text{Cl}(\text{NH}_3)_4]^{4+}$ (Foong, S. W.; Mast, R. D.; Stevenson, M. B.; Sykes, A. G. *J. Chem. Soc. A* **1971**, 1266–1273).

Ministry of Education, Science, and Culture of Japan. The authors are indebted to Dr. Yoshinori Hasegawa, College of General Education, Tohoku University, for the use of apparatus.

Registry No. $(\Delta\Delta, \Lambda\Lambda)-[(en)_2Co^{III}(\mu-OH)(\mu-O_2^{2-})Co^{III}(en)_2]^{3+}$,

36885-26-4.

Supplementary Material Available: Table I, observed rate constants for the decomposition reaction (1 page). Ordering information is given on any current masthead page.

Contribution from the Laboratory for Electron Spectroscopy and Surface Analysis, Department of Chemistry, University of Arizona, Tucson, Arizona 85721

Comparison of Thionitrosyl and Nitrosyl Bonding in Dicarbonyl(η^5 -cyclopentadienyl)chromium Complexes by Gas-Phase Ultraviolet and X-ray Photoelectron Spectroscopy

DENNIS L. LICHTENBERGER* and JOHN L. HUBBARD

Received November 2, 1984

The gas-phase He I/He II UPS and Mg K α XPS data for the compounds $(\eta^5-C_5H_5)Cr(CO)_2NO$ and $(\eta^5-C_5H_5)Cr(CO)_2NS$ are reported. The first ionization potentials for the two complexes are nearly the same (nitrosyl 7.56 eV; thionitrosyl 7.47 eV), contrary to indications from mass spectrometry appearance potentials. A short C–O stretching progression (ca. 2000 cm^{-1}) in the first ionization band of the nitrosyl compound shows that it is predominantly associated with metal d character and is symmetrically π delocalized into the carbonyls. This orbital is primarily of δ symmetry with respect to the NO or NS ligand. The next two ionizations for both complexes, which complete the formal d^6 configuration at the metal, are sensitive to the π symmetry interaction with the NO or NS group. These ionizations are approximately degenerate for the NO complex and are stabilized by nearly 1 eV relative to the first band as a consequence of the stronger Cr–NO π -back-bonding relative to Cr–CO back-bonding. These ionizations are slightly destabilized and are sharper for the NS complex relative to the NO complex, showing stronger metal π interaction with both the NS π bond and π^* orbitals. The dramatic loss of intensity of these ionizations in the He II spectrum of the thionitrosyl complex experimentally demonstrates significant delocalization with both the NS π -donor and π -acceptor levels to give large NS (sulfur) character for these ionizations. The nitrogen 1s binding energy for the NS complex is almost 2 eV lower than that for the NO complex, suggesting a much more negative charge on the NS nitrogen. In contrast, the chromium, carbon, and oxygen core binding energies do not differ significantly between the two complexes. A formal potential model analysis of the (Cr–N–O) and (Cr–N–S) XPS shifts indicates a slightly more positive metal in the NS complex. These results are in agreement with Fenske–Hall approximate calculations and with other physical properties of the two compounds.

Introduction

The discovery by Legzdins and co-workers¹ of the volatile thionitrosyl complex $(\eta^5-C_5H_5)Cr(CO)_2NS$ has provided an excellent opportunity to compare the ligating and other physical-chemical properties of NS with those of NO in its isoelectronic and nearly isostructural analogue, $(\eta^5-C_5H_5)Cr(CO)_2NO$. The IR, mass spectral, and certain NMR properties have been examined by Legzdins and co-workers, and the results apparently present an "interesting dichotomy" between the ligating abilities of NO and NS in these molecules.¹ Although the mass spectral fragmentation data and the infrared data suggested that the NS ligand is more strongly bound to the metal and is a better remover of metal electron density than NO, their appearance potential data and NMR shifts suggested on first principles that the metal is more electron rich in the thionitrosyl complex. We have reported the results of a valence He I study of the nitrosyl and thionitrosyl complexes² and subsequently discussed the counterintuitive aspects of CS and NS coordination, which arises from their ability to act as both strong π donors and π acceptors to the metal.³ More recently we have provided a complete heteronuclear NMR study of pairs of nitrosyl/thionitrosyl complexes of chromium, molybdenum, and tungsten.^{4,5}

The previous ionization studies of these complexes were limited to valence He I photoelectron spectroscopy and comparison with approximate molecular orbital calculations. A clear and more complete understanding of these systems is available from a combination of gas-phase He I/He II UPS valence ionization information and gas-phase Mg K α XPS core ionization data. As opposed to core-only or valence-only studies, the combined valence/core ionization analysis allows an effective separation of effects of charge distribution from the effects of bonding and/or electron relaxation.⁶ This is particularly important in the com-

parison of NS with NO. Of special interest is the relationship between specific σ and π interactions and the charge distribution around the metal. When oxygen is replaced by a less electronegative sulfur atom the increase in negative charge at nitrogen will effectively increase the σ -donor ability of the ligand. Therefore, the change of charge on the nitrogen atom, and consequently on the metal atom, is of special importance. Also, like CS, the NS ligand is expected to be a considerable π donor to the metal as well as a good π acceptor.⁷ The XPS analysis allows us to assess the net effect of these bonding interactions on the distribution of charge in the molecule.

Comparison of the ionizations of the $CpCr(CO)_2NO$ complex ($Cp = \eta^5-C_5H_5$) with those of $CpMn(CO)_3$ also allows measurement of the electronic effects of formally moving a proton from the metal to one of the carbonyls, i.e. transforming a $(Mn-CO)^+$ unit to a $(Cr-NO)^+$ unit while leaving the rest of the coordination environment essentially unchanged. Compared to that in the $CpMn(CO)_3$ and $CpMn(CO)_2CS$ complexes, where the metal d^6 ionizations (arising from a perturbed t_{2g} set in strict octahedral symmetry) were closely overlapping, this "proton" perturbation distorts the pseudo-octahedral electronic symmetry around the metal to pseudo- C_{4v} symmetry, thus separating the metal orbital with δ symmetry from the metal orbitals with π symmetry to the NO or NS group. This convenient δ - π separation allows observation of the difference between Cr–NO and Cr–NS π mixing by the measurement of the He I/He II cross section

* To whom correspondence should be addressed.

- (1) Greenhough, T. J.; Kolthammer, B. W. S.; Legzdins, P.; Trotter, J. *Inorg. Chem.* **1979**, *18*, 3548.
- (2) Hubbard, J. L.; Lichtenberger, D. L. *Inorg. Chem.* **1980**, *19*, 1388.
- (3) Hubbard, J. L.; Lichtenberger, D. L. *Inorg. Chem.* **1980**, *19*, 3865.
- (4) Lichtenberger, D. L.; Hubbard, J. L. *Inorg. Chem.* **1984**, *23*, 2718.
- (5) Minelli, M.; Hubbard, J. L.; Lichtenberger, D. L.; Enemark, J. H. *Inorg. Chem.* **1984**, *23*, 2721.
- (6) Jolly, W. L. *Acc. Chem. Res.* **1983**, *16*, 370.
- (7) Lichtenberger, D. L.; Fenske, R. F. *Inorg. Chem.* **1976**, *15*, 2015.